Neurobiology of Disease

Neuronal PPARγ Deficiency Increases Susceptibility to Brain Damage after Cerebral Ischemia

Xiurong Zhao,[1] **Roger Strong,**[1] **Jie Zhang,**[1] **Guanghua Sun,**[1] **Joe Z. Tsien,**[2] **Zhenzhong Cui,**[3] **James C. Grotta,**[1] **and Jaroslaw Aronowski**[1]

[1]Stroke Program, Department of Neurology, University of Texas, Houston, Medical School, Houston, Texas 77030, [2]Brain and Behavior Discovery Institute, Medical College of Georgia, Augusta, Georgia 30912, and [3]Section on Neural Gene Expression, National Institute of Mental Health–National Institutes of Health, Bethesda, Maryland 20892

Peroxisome proliferator-activated receptor gamma (PPARγ) plays a role in regulating a myriad of biological processes in virtually all brain cell types, including neurons. We and others have reported recently that drugs which activate PPARγ are effective in reducing damage to brain in distinct models of brain disease, including ischemia. However, the cell type responsible for PPARγ-mediated protection has not been established. In response to ischemia, PPARγ gene is robustly upregulated in neurons, suggesting that neuronal PPARγ may be a primary target for PPARγ-agonist-mediated neuroprotection. To understand the contribution of neuronal PPARγ to ischemic injury, we generated conditional neuron-specific PPARγ knock-out mice (N-PPARγ-KO). These mice are viable and appeared to be normal with respect to their gross behavior and brain anatomy. However, neuronal PPARγ deficiency caused these mice to experience significantly more brain damage and oxidative stress in response to middle cerebral artery occlusion. The primary cortical neurons harvested from N-PPARγ-KO mice, but not astroglia, exposed to ischemia *in vitro* demonstrated more damage and a reduced expression of numerous key gene products that could explain increased vulnerability, including SOD1 (superoxide dismutase 1), catalase, glutathione *S*-transferase, uncoupling protein-1, or transcription factor liver X receptor-α. Also, PPARγ agonist-based neuroprotective effect was lost in neurons from N-PPARγ neurons. Therefore, we conclude that PPARγ in neurons play an essential protective function and that PPARγ agonists may have utility in neuronal self-defense, in addition to their well established anti-inflammatory effect.

Introduction

The peroxisome proliferator-activated receptors (PPARs), including α, γ, and δ/β encoded by separate genes, are members of the nuclear receptor superfamily of ligand-activated transcription factors (Kliewer et al., 1994; Mangelsdorf et al., 1995; Chinetti et al., 2000; Berger and Moller, 2002). Normally, PPARγ regulates gene transcription by binding to conserved DNA sequences termed PPRE (peroxisome proliferator response elements), as heterodimers with retinoic X receptor. Agonists of PPARγ include fatty acids, nonsteroidal anti-inflammatory drugs (Lehmann et al., 1995) naturally occurring 15d-Δ^{12,14}-PGJ$_2$ (Forman et al., 1995; Kliewer et al., 1995; Ricote et al., 1998; Rohn et al., 2001), and a class of synthetic compounds, thiazolidinediones (Stumvoll and Häring, 2002). PPARγ was originally characterized in adipose tissue as a regulator of lipid and glucose metabolism; however, new evidence indicates that PPARγ is present in most cell types where it mediates multimodal function (Giannini et al., 2004). Recently, PPARγ was identified also in neurons, but its function here is less clear. Activators of PPARγ, including 15d-PGJ$_2$ or thiazolidinediones administered to ani-

mals before or after the onset of ischemia, reduce ischemic damage (Shimazu et al., 2005; Sundararajan et al., 2005; Ou et al., 2006; Victor et al., 2006; Tureyen et al., 2007). The reduction of proinflammatory responses, antiatherosclerotic activities, and antioxidant effect was proposed as mechanisms underlying the beneficial effect of PPARγ activators (Jiang et al., 1998; Chinetti et al., 2000; Giannini et al., 2004; Pereira et al., 2005; Sundararajan et al., 2005; Zhao et al., 2005). We and others demonstrated that PPARγ activators protect neurons in culture from NMDA-induced cytotoxicity (Uryu et al., 2002; Zhao et al., 2006b), suggesting that PPARγ protects brain from ischemia via mechanisms that directly target neurons and are independent from inflammation or other extrinsic factors. In non-neuronal tissues, PPARγ promotes expression of numerous gene products whose profile of activity could be linked to oxidative stress suppression, proper mitochondrial function, or lipid and glucose metabolism and transport (Yoo et al., 1999; Akiyama et al., 2002; Girnun et al., 2002; Dello Russo et al., 2003; Romera et al., 2007). Assuming neural tissue could use PPARγ in a similar manner to that of non-neuronal cells, a functional PPARγ in neurons could act to protect neurons from damage.

Here, to assess the role of neuronal PPARγ in susceptibility to ischemic injury, we generated neuron-specific PPARγ null mice by using the Cre–loxP technology and taking advantage of α-Ca^{2+}/calmodulin-dependent protein kinase II (αCaM–KII) promoter to achieve neuronal specificity (Kelly et al., 1987; Tsien et al., 1996). These mutant mice were subjected to ischemic injury

Table 1. Primer sequence for genotyping

Gene name	Primer sequence	Usage	Product size	PCR condition
CaM–KII–Cre	F: 5′-GGGAGGTAGGAAGAGCGATG B: 5′-CCATGAGTGAACGAACCTGG	Genotyping CaM–KII–Cre mice	1200∼1500 bp	94℃ (2 min), 65℃ (50 s), and 72℃ (1.5 min), 30 cycles
PPARγ^fl/fl	F: 5′-TGTAATGGAAGGGCAAAAGG B: 5′-TGGCTTCCAGTGCATAAGTT	Genotyping PPARγ^fl/fl mice	214 bp (WT) and 250 bp (Lox-P)	94℃ (1 min), 55℃ (30 s), and 72℃ (30 s), 30 cycles
Recombinant PPARγ	F: 5′-GTCACGTTCGACAGGACTGTGTGAC B: 5′-TATCACTGGAGATCTCCGCCAACAGC	Genotyping N-PPARγ-RO mice	700 bp (full) and 400 and 300 bp (recombinant)	94℃ (1 min), 55℃ (30 s), and 72℃ (50 s), 35 cycles

WT, Wild type; F, forward; B, backward.

using unilateral middle cerebral/common carotid artery occlusion. We also generated neuronal cultures from these mice to capture changes in gene expression in neurons as a consequence of PPARγ deletion. Our study revealed that neuronal PPARγ deficiency is associated with augmented ischemic damage, as judged by both morphological and functional assays. In addition, neurons from PPARγ mutant mice demonstrated impaired expression of many prosurvival gene products and suffered more damage including oxidative stress when subjected to ischemia *in vitro*.

Materials and Methods

Animals. All experiments were performed in 3–6-month-old male and female mice. All animals were congenic with the C57BL/6 strain. Mice were fed standard mouse diet and housed in standard mouse cages on a 12 h inverted light/dark cycle. Behavioral analyses were performed between 10:00 A.M. to 4:00 P.M. For measurement of mouse body weight, food intake, and cerebral blood vasculature, data were collected and compared within littermates. Blood glucose was determined on whole venous blood by using an automatic glucometer (One Touch Basic; Lifescan). All experimental procedures were approved by the Institutional Animal Care Committee of University of Texas Health Science Center at Houston.

Generation of neuronal-specific PPARγ mutant mice. Floxed (fl) PPARγ (PPARγ^fl/fl) mice (B6.129-*Pparg^tm2Rev*; The Jackson Laboratory; stock # 004584) were crossed with αCaM–KII–Cre mice (Cui et al., 2005) to generate neuronal-specific PPARγ knock-out mice, αCaM–KII–Cre/PPAR^f/f (N-PPARγ-KO). Specifically, we used the Tg-62-Cre line containing a 6.2Kb of αCaM–KII promoter region (Cui et al., 2004). The αCaM–KII gene is known to confer neuron-specific expression with tissue-selectivity predominantly in the adult forebrain, including hippocampus, cortex and caudate–putamen (Kelly et al., 1987; Olson et al., 1995; Tsien et al., 1996). Therefore, by placing Cre cDNA under the control of αCaM–KII promoter, neuronal-specific Cre expression could be achieved (Tsien et al., 1996). The PPARγ^fl/fl mice have two loxP sites introduced on either side of the exons 1 and 2 of PPARγ. Cre-mediated deletion of exon 1 and 2 result in loss of PPARγ (He et al., 2003). Specifically, to generate N-PPARγ-KO, αCaM–KII–Cre mice were first crossed with PPARγ^fl/fl mice to generate αCaM–KII–Cre/PPAR^f/+ mice (approximately half of the progenies produced from these crosses). Second, αCaM–KII–Cre/PPAR^fl/+ mice were again mated with PPARγ^fl/fl mice to generate N-PPARγ-KO mice. This second crossing served to delete both copies of the PPARγ alleles in αCaM–KII–Cre-expressing neurons. Both PPARγ^fl/fl and αCaM–KII–Cre mice were maintained on a C57BL/6 genetic background for at least six generations. PPARγ^fl/fl mice were used as the control. Three- to six-month-old animals were used in the *in vivo* experiments, and 1-d-old postnatal pups (p1) were used in the tissue culture experiments.

Genotyping. The genotyping for determining αCaM–KII–Cre transgenic, PPARγ–LoxP and N-PPARγ-KO mice was performed by PCR method. The primer sequence and PCR condition is listed in Table 1. The expression of Cre and recombinant PPARγ in N-PPARγ-KO mice or in the cultured neurons was tested with reverse transcriptase (RT)-PCR. The primer sequence and PCR condition is listed in Table 2. In testing the recombinant PPARγ in the N-PPARγ-KO mice, the primer pair listed in Table 2 amplifies a full PPARγ band at 700 bp and two recombinant

PPARγ bands at 400 and 300 bp. The 300 bp band has the exact sequence predicted from the deletion of the loxP-flanked region. The 400 bp product is identical to the 300 bp product, except that an additional 100 bp of intronic sequence from the intron three of PPARγ was spliced into the transcript (Hevener et al., 2003).

LacZ staining to detect the Cre expression pattern. Mice carrying Tg–Cre were crossed with β-actin promoter loxP–stoploxP–LacZ transgenic mice as we described previously (Cui et al., 2005).The double transgenic mice (carrying Tg–Cre and Tg–LacZ) were examined at 25 d old. The staining procedure using X-gal solution was performed exactly as we described previously (Cui et al., 2005).

Ischemia model in mice. In this experiment, we used 3–6-month-old animals. Focal ischemia was induced by left middle cerebral artery (MCA) and left common carotid artery (CCA) occlusion, as we described previously (Aronowski et al., 2000). Briefly, all animals were fasted overnight with *ad libitum* access to water and then anesthetized with 0.35 g/kg i.p. injection of chloral hydrate. A single injection of chloral hydrate provided 2 h of continuous anesthesia. The rectal temperature was monitored and maintained at 36.5 ± 0.5℃ during ischemia and the first hour of reperfusion using a feedforward temperature controller (YSI Model 72) using a heating lamp and warming blanket. An incision was made through the left temporalis muscle perpendicular to a line drawn between the external auditory canal and the lateral canthus of the left eye. Under direct visualization with a surgical microscope, a burr hole was drilled at 1.5 mm rostral to the fusion of the zygomatic arch with the squamosal bone to expose the left MCA rostral to the rhinal fissure. A 0.005 inch diameter stainless steel wire (Small Parts) was placed underneath the left MCA rostral to the rhinal fissure, proximal to the major bifurcation of the MCA, and distal to the lenticulostriate arteries. The artery was then lifted and the wire rotated clockwise. The CCA was occluded using atraumatic Heifetz aneurysm clips. Reperfusion after 60 min of occlusion is established by first removing the aneurysm clip from the CCA and then rotating the wire counterclockwise and removing it from beneath the MCA. Interruption of flow through the MCA was inspected under the microscope and verified by cerebral perfusion (CP) measurement using a laser Doppler flowmeter (LDF, model BPM2; Vasamedics). We used LDF to monitor CP at baseline (before occlusion), during MCA/CCA occlusion (at 5 and 55 min from the onset of occlusion), as well as during reperfusion (5 min after reversal of occlusion). The CP was collected by placing LDF probe on the surface of the skull at the location (3.5 mm caudal and 1.5 mm laterally to the bregma) that representing the ischemic penumbra.

Infarction volume measurement. The infarction volume was measured as we described previously (Aronowski et al., 1997). Briefly, the mice were deeply anesthetized by intraperitoneal injection of 0.6 g/kg of chloral hydrate; intracardiac perfusion with 40 ml of ice-cold PBS was performed before animals were decapitated. The brain was removed and sliced into 2 mm coronal sections using a plastic mold. The sections were stained with 2% 2,3,5-triphenyltetrazolium chloride (TTC) for 30 min at room temperature and fixed in 10% formalin. The image of each section was digitized, and the infarction volumes were determined morphometrically using NIH ImageJ software. Infarcts produced by our protocol are restricted to cortical tissue. The infarct volume (mm^3) was calculated from the difference between the volume of contralateral cortex and the volume of the TTC-stained (nonischemic) portion of ipsilateral cortex of each rat. This indirect measure of infarct volume, based on the assumption that the volume of the ipsilateral and contralateral cortex are the

Table 2. Primer sequence for RT-PCR

Gene name	Primer sequence	Seqence ID	Cycle #	Product size (bp)
Cre	F: GCATTACCGGTCGATGCAACGAGTG	AF234173.1	30	374
	B: GAACGCTAGAGCCTGTTTTGCACGTTC			
PPARγ	F: TTCTCAGACTCGAAGCAGCA	NM_013672	35	346
	B: CACAACATACTGCCCACCAG			
SOD1	F: AGGCTGTACCAGTGCAGGAC	X 06683	28	300
	B: GTTTACTGCGCAATCCCAAT			
CAT	F: CCTCGTTCAGGATGTGGTTT	X 52108	32	325
	B: GGCATCCCTGATGAAGAAAA			
GST	F: AAGACTGCCTTGGCAAAAGA	NM_029555	26	345
	B: GCCAGTATCTGTGGCTCCAT			
UCP-1	F: TCTCAGCCGGCTTAATGACT	NM_009463	32	445
	B: GTCGGTCCTTCCTTGGTGTA			
LXRα	F: GGATAGGGTTGGAGTCAGCA	NM_013839	26	347
	B: GCAGGACTTGAGGAGGTGAG			
LPL	F: GCTGGCCTTGAACTCTCAAC	NM_008509	28	379
	B: CGGCAACAATCCTGGTACTT			
GAPDH	F: TGTTCCTACCCCCAATGTGT	NM_001001303	22	396
	B: TGTGAGGGAGATGCTCAGTG			
SYNP	F: AGACAGGCAGGTGAAGAGGA	NM_009305	20	483
	B: GGGCCACAGTCAGACAAAAT			
EAAT2	F: TCTGAGGAGGCCAATACCAC	NMMU11763	30	312
	B: GTCCTTGATGGCGATGATCT			

F, Forward; B, backward.

same before ischemia, corrects the total infarct volume for the edema component (Swanson et al., 1990).

Neurological dysfunction analysis. All behavioral tests in mouse were conducted in a quiet and low-lit room by an experimenter blinded with respect to the treatment groups. Pretests were conducted to exclude abnormally behaving animals. A combination score from a battery of behavioral tests (footfault, forelimb placing, postural reflex, and cylinder tests) to measure the neurological functional deficits was used as we reported previously (Zhao et al., 2007a).

Primary cortical neuron cultures. The neuronal culture was generated from cortices of littermates (within 24 h after birth) of N-PPARγ-KO and the control (LoxP) mice. First, the cortices were dissected and dissociated by trituration as we described previously (Zhao et al., 2006b). The dissociated cells were plated on poly-L-lysine-coated culture plates in neurobasal medium with B27 at a cell density of 300–700/mm^2. The cells were maintained in a CO$_2$ incubator (5% CO$_2$) at 37.0 ± 0.5°C. After 24 h in culture, the cells were treated for 48 h with 0.1 μM cytosine arabinoside (Ara–C) to inhibit glial growth. After 15 d in culture, the cells form extensive axonal and dendritic networks and are ready for the experiments. The expression of Cre and PPARγ in those neuronal cultures was determined at 5, 9, and 15 d after being in culture *in vitro*.

Primary glial cultures. The primary glial cultures were prepared using the same methods as we described in the neuronal cultures except that the cells were cultured in DMEM plus 10% fetal bovine serum without Ara–C. After 15 d in culture, the cells were subjected to a shaking procedure at 220 rpm for 2 h to remove the neurons. The closely attached glial cells were used as the glia-enriched cells for measurement of the cell specificity to the oxygen–glucose deprivation (OGD) injury.

Determination of lactate dehydrogenase activity. The release of lactate dehydrogenase (LDH) into the culture medium was measured using a spectrophotometer and an LDH assay kit (Promega) as we described previously (Zhao et al., 2006b).

Immunohistochemistry and neuronal counting. The cultured neurons grown on German Glass were either fixed in 4% paraformaldehyde at room temperature for 10 min (DAB staining) or were treated with 95% methanol containing 5% acetic acid at −15°C for 10 min. Immunostaining of microtubule associated protein (MAP2), Cre, NeuN, or glial fibrillary acidic protein (GFAP) was performed by incubating cells with (1) rabbit polyclonal antibody for MAP2 (1:1000; Sigma-Aldrich for DAB), (2) chicken polyclonal antibody for MAP2 (1:1000; Abcam; immunofluorescence), (3) rabbit polyclonal antibody for Cre (Novagen; 1:1000), (4)

goat polyclonal antibody for GFAP (1:1000), and (5) mouse monoclonal for NeuN (Millipore Bioscience Research Reagents; 1:1000) at 4°C for overnight. The MAP2 signal was visualized with a goat anti-rabbit ABC Elite kit (Vector Laboratories) followed by DAB (Vector Laboratories). The goat anti-rabbit IgG–Alexa Fluor 488, rabbit anti-goat IgG–Alexa Fluor 546, goat anti-mouse IgG–Alexa Fluor 488 or goat anti-chicken IgG–Alexa Fluor 546 (all at 1:100; Invitrogen) were used to visualize the remaining antigens using a protocol we described previously (Zhao et al., 2006b). The Hoechst 33258 (1 μg/ml; Invitrogen) was applied to stain the nuclei. The staining was captured using a Zeiss Axioscop 2 photomicroscope equipped with a motorized stage and CoolSnap ES (Photometrics) camera driven by MetaMorph software.

We used 10-μm-thin cryosections of brains to stain for NeuN as we described previously (Felberg et al., 2002). The immunofluorescence images in three preselected areas of the cerebral cortex and dentate gyrus of hippocampus (same anatomical location was used for each animal) were recorded. The neurons (NeuN-positive cells) were counted using a MetaMorph program set for recognition of fluorescent pixels (immunofluorescent cells). Each area subjected to neuronal counting was set as 300 × 300 μm. Six areas were counted per each animal. Three animals from each group were used for the analyses.

OGD injury model. Thirteen- to fifteen-day-old primary cortical neurons or glia in culture were subjected to OGD exactly as we reported previously (Kim et al., 2004). Briefly, the culture media were replaced with the neurobasal medium without glucose, and the cultures were placed in a gas-tight humidified chamber filled with 5% CO$_2$/95% N$_2$ for 1 h for neurons and 2 h for glia. At the end of OGD, the cultures were returned to their original culture condition and maintained for 24 h. In the experiment using rosiglitazone (0.5 μM final concentration), the compound was added to culture media 30 min before induction of OGD and then maintained in the media during the entire recovery period.

Oxidative stress measurement. Oxidative stress in the cultured neurons was measured by assessing the oxidative damage to protein and lipid, as we reported previously (Zhao et al., 2007b). Briefly, samples containing 2 μg proteins of cell lysates were spotted on a nitrocellulose membrane using the Bio-Rad Dot Blot system. After air drying, the membranes were probed with anti-nitrotyrosine (3′-NT; Upstate Biotechnology; 1 μg/ml) and anti-4-hydroxynone (4-HNE; Millipore Bioscience Research Reagents; AB5605) antibodies to measure the oxidative damage to proteins and lipids, respectively. The blots were incubated in goat anti-rabbit–HRP (1:5000) for 45 min, and the antibodies were visualized with en-
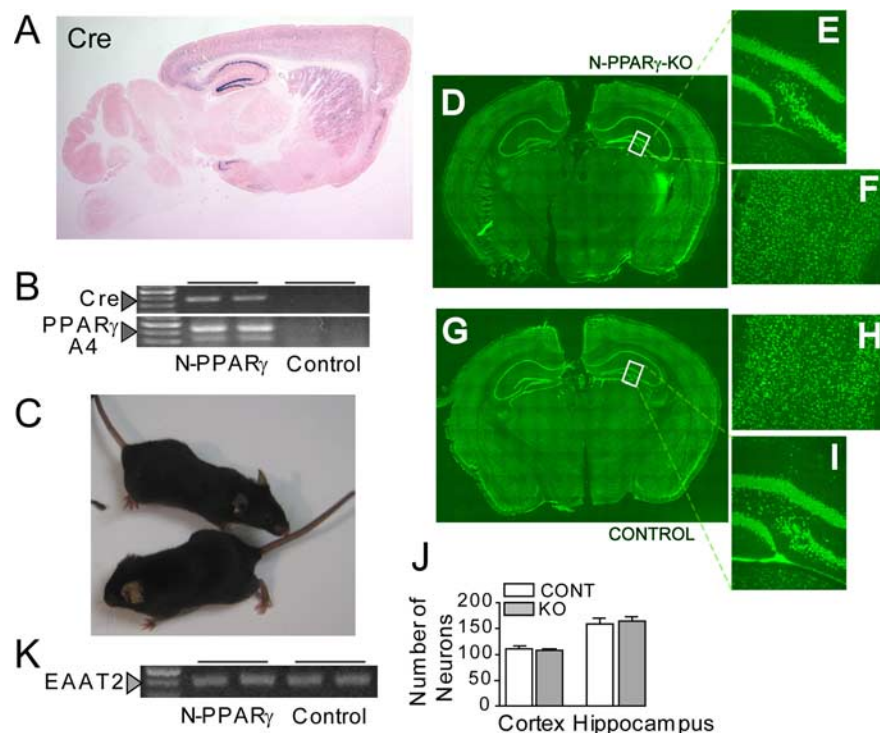
Figure 1. **A**, Photograph of LacZ staining in the Tg-62–Cre mouse showing the Cre/LoxP recombination pattern. A sagittal section shows that the Cre/loxP recombination (indicated by blue X-gal signals) is restricted to the forebrain regions and primarily the cerebral cortex, striatum, and hippocampus. Eosin was used for counterstain. **B**, Detection of mutant PPARγ mRNA by RT-PCR analysis. Messenger RNAs for the Cre and PPARγ were isolated from cerebral cortex of N-PPARγ-KO and LoxP (Control) mice at 3 months of age. Arrowheads indicate presence of Cre products (top) and recombined 300 bp and 400 bp PPARγ PCR products (bottom) (see Materials and Methods for more details). Note that expression of Cre corresponds with the appearance of unique RT-PCR bands specific to the recombined fragments of PPARγ. **C**, Both the control (bottom of the picture) and N-PPARγ-KO mice have normal appearance. **D**, The NeuN immunofluorescence (green) demonstrates neuronal density and distribution in N-PPARγ-KO (**D–F**) and the control (**G–I**) mice. Coronal section through a whole brain (**D, G**), hilus of dentate gyrus (**E, I**), and cerebral cortex (**F, H**) of representative mice at 3 months of age are shown. **J**, Summary bar graph illustrating neuronal (NeuN-positive cells) count in the cerebral cortex and in denature gyrus of hippocampus of Lox-P (control; CONT) and N-PPARγ-KO (KO) mice. Each count covered a 300 × 300 μm area. Data are expressed as mean ± SEM ($n = 6$ fields counted in 3 animals). **K**, Expression of astroglia-specific PPARγ gene target, EAAT2, is not affected in cortex of N-PPARγ-KO, compared with control mice, confirming neuronal specificity of the knockout.

hanced chemiluminescence (Pierce). Semiquantification of the signal on x-ray film was achieved by analyses of optical density using a computer-assisted Kodak Analysis (EDAS 290).

Neurofilament degradation. Cell lysates (20 μg) from 15-d-old control and N-PPARγ-KO-cultured neurons (generated from the cerebral cortices) at 24 h after 1 h of OGD were subjected to SDS-PAGE and followed by Western blotting. Rabbit anti-neurofilament (NF)-M and NF-L antibodies (Abcam) were used as we described previously (Aronowski et al., 1999). Immonopositive bands representing NF-M and NF-L were semiquantified using densitometrical analysis, EDAS 290 system.

RT-PCR. The mRNA levels were semiquantified by RT-PCR as we reported previously (Zhao et al., 2007a). We used mouse glyceraldehyde-3-phosphate dehydrogenase (GAPDH) gene as an internal control. Each set of PCRs included the control samples run without RNA, or the RT step was omitted to ensure that PCR products resulted from amplification of the purified mRNA rather than of genomic DNA. The cycle number corresponding to the exponential amplification phase was determined individually for each gene and each preparation by the cycle-product curve. The sequences of primers and cycle number accepted for quantification are listed in Table 2. The PCR products were run on 1–2% agarose gels and stained with ethidium bromide. The image was digitized, and the optical density of each band was quantified using a computer-assisted Kodak Analysis (EDAS) 290 system. The data (optical density) were first normalized by internal control (GAPDH) and then expressed as percentage change over the vehicle control.

Statistical analysis. All data were expressed as mean ± SEM. For *in vitro* experiments, we pooled the samples from three culture wells and repeated the experiments three times, unless otherwise stated in the figure legends. We performed statistical analyses with GraphPad and InStat programs. We used one-way ANOVA followed by the Newman–Keuls post-test for multiple comparison. Nonpaired *t* test was used when two groups were compared. Differences are considered significant if $p \leq 0.05$.

Results

N-PPARγ-KO mice

To study PPARγ in neurons, we generated N-PPARγ-KO mice using Cre–loxP recombination system. To achieve neuronal selectivity in PPAR deletion, we crossed PPARγ^fl/fl mice with mice expressing Cre under a well characterized αCaM–KII promoter to drive Cre expression (Olson et al., 1995; Tsien et al., 1996; Cui et al., 2005). Here, we specifically used a Tg–Cre-62 line of mice which allows Cre–loxP-mediated recombination to be completed by the third postnatal week and to be confined to the cortex, striatum, and hippocampus in the forebrain (Fig. 1A illustrates the Cre–loxP recombination pattern with lacZ staining) (Tsien et al., 1996; Cui et al., 2005). As expected, we determined a strong presence of Cre expression and an abundance of Cre-mediated recombination of *PPARγ-flox* allele in tissue samples from the cerebral cortex of N-PPARγ mice, as determined at 3 months of age (Fig. 1B).

The N-PPARγ-KO mice have normal appearance (Fig. 1C) and seem to be normal with respect to their gross brain structures, as determined by visually inspecting neurons in both the hippocampus and cerebral cortex (Fig. 1D,G). The hippocampal (Fig. 1E) and cortical (Fig. 1F) neurons in N-PPARγ-KO mice seem morphologically intact and demonstrate similar neural architecture/anatomy (Fig. 1H,I) and density (Fig. 1J) to the control mice, indicating that PPARγ deficiency alone is not sufficient to cause neuronal loss or defective brain development. This notion is further supported by a similar low abundance of TUNEL-positive cells or apoptosis-like morphology in the Hoechst-stained nuclei in cerebral cortex or hippocampus of N-PPARγ-KO mice, as determined at 1, 3, and 6 months of age (data not included). It is likely that N-PPARγ mutation did not affect PPARγ activity in astroglia, as the expression of excitatory amino acid transporter 2 (EAAT2) that is known to be under the control of PPARγ and expressed mainly in astrocytes (Romera et al., 2007) was not affected in the forebrain of N-PPARγ-KO (Fig. 1K).

The neuronal PPARγ deficiency did not impact animal growth and body weight (suggestive of intact metabolism), body temperature, daily behavioral activity, brain vascular anatomy and reproducibility, as determined by examining the mice for up to 6 months after birth. There were no differences in blood glucose, blood pressure, and plasma ions (Na^+, K^+, Ca^{2+}, Cl^-, $NaHCO^-$) compositions between the neuron-PPARγ-KO and

the control mice (data not shown). At 5 months of age, body weight of N-PPARγ-KO and control mice were similar and were 24.7 ± 2.4 g ($n = 8$) versus 24.1 ± 3.9 g ($n = 8$), respectively.

N-PPARγ-KO mice are more susceptible to focal cerebral ischemia

At ~3–6 months of age, randomly selected male and female N-PPARγ-KO mice and age- and sex-matched littermate controls were subjected to a transient 60 min MCA/CCAo followed by 3 d of reperfusion. The damage produced with this ischemia method is restricted to the cortical tissue, overlapping with the distribution of Cre expression. In response to ischemia, N-PPARγ-KO mice developed 40% larger infarction, compared with control mice (28.9 ± 4.5 mm^3 vs 17.4 ± 2.3 mm^3 infarct volume) (Fig. 2A,C). The increased vulnerability to ischemic damage was most likely not dependent on gender, as both male and female N-PPARγ-KO mice demonstrated either strong trend (males) or statistical difference (females) toward increased vulnerability to ischemic damage (Fig. 2B). The larger volume of infarction in N-PPARγ-KO mice coincided with increased neurological dysfunction (NDS) (Fig. 2D), indicating a close association between the volume of histological damage and neurological deficit.

The increased vulnerability to ischemic damage was likely not attributable to changes in CP as the values of perfusion in N-PPARγ-KO mice at baseline (before occlusion), during ischemia, and during reperfusion were indistinguishable between N-PPARγ-KO and control mice (Fig. 2E).

Finally, there was no difference in surgery/stroke-related mortality between N-PPARγ-KO and control mice. The mortality was 26 and 29% for the control and knock-out group, respectively. All deaths occurred within the first 24 h after the stroke.

Primary neurons from N-PPARγ-KO mice show reduced expression of PPARγ and PPARγ-dependent genes

To better understand the profile and consequences of PPARγ deletion in neurons, we used primary neuron-glia coculture or neuron-enriched culture system and N-PPARγ-KO mice as a source of PPARγ null neurons. Earlier published studies demonstrated that the activity of αCaM–KII promoter is barely detectable at day 4 postnatal but is increased as much as tenfold by day 16 (Scholz et al., 1988; Burgin et al., 1990). In agreement with this study, the αCaM–KII promoter activity in neurons, as measured by Cre mRNA expression, was negligible for up to 9 d (Fig. 3A), followed by a robust increase at day 15. Additionally, Cre protein expression was confined to the nuclei, as determined using immunoreactivity for Cre protein in the neuron/glia coculture system (Fig. 3B). Further studies using double immunostaining for Cre and cell-specific marker demonstrated that Cre colocalizes to nuclei of neurons (NeuN-positive cells) (Fig. 3C) but not astroglia (GFAP-positive cells) (Fig. 3D). The Cre expression in cultured neurons coincided with significant loss of PPARγ protein
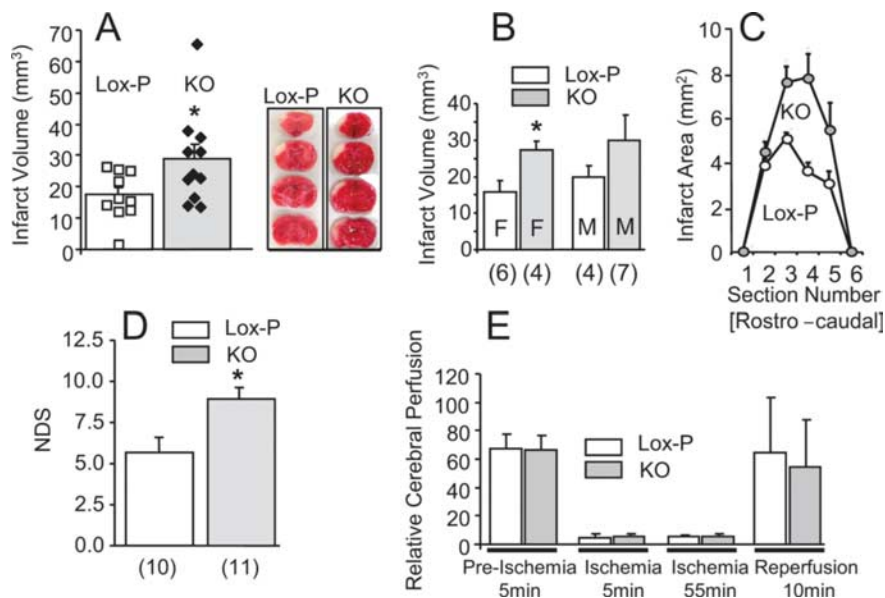

Figure 2. Neuronal PPARγ deficiency aggravates cerebral ischemic damage. N-PPARγ-KO (KO) and control (Lox-P) mice were subjected to reversible 60 min MCA/CCA occlusion. A, The infarct volumes representing composite of all the control (white filling) and KO (gray filling) mice (individual mice are indicated as squares or diamonds within each group), (B) segregated by gender (M, male; F, female; number below each bar indicates the sample size), *$p < 0.05$, and infarct areas (C) at six rostrocaudal plains were determined from morphometric analyses of TTC-stained brain sections at 3 d after the onset of ischemia. Representative photographs of TTC-stained brain sections demarcate infarcts in control (Lox-P) and N-PPARγ-KO (KO) mice (included in A). Infarct volume in all groups was established at 3 d after ischemia. D, Bar graph illustrating the NDS as measured at 3 d after ischemia using a battery of behavioral tests. Number below each bar indicates the sample size. *$p < 0.05$. E, Bar graph illustrating cerebral perfusion values in the peri-ischemic areas of control ($n = 10$) and N-PPARγ-KO mice ($n = 11$) at four time points representing 5 min before ischemia (Preischemia; baseline), 5 min and 55 min after induction of ischemia, and 10 min after reversal of the occlusion (reperfusion) measured using Laser Doppler flowmetry. The results are presented as mean ± SEM.

(Fig. 3E), demonstrating that it is possible to induce PPARγ gene knockdown in neurons using αCaM–KII promoter-driven Cre expression.

In agreement with the consequences of deficient PPARγ expression in neurons, we observed significant reduction in PPARγ-dependent gene expression (Fig. 3F,G), as studied in 15-d-old cultured cortical neurons. These included genes encoding for enzymes involved in neutralization of reactive oxygen radicals, such as Cu, Zn-superoxide dismutase (SOD1), catalase, and glutathione S-transferase (GST), enzyme involved in proper functioning of mitochondria, uncoupling protein-1 (UCP-1), enzymes involved in lipid metabolism, lipoprotein lipase (LPL), and transcription factor liver X receptor-α (LXRα). Although we detected reduction in the expression of canonical PPARγ gene products, there was no change in expression in GAPDH or synaptophysin genes. This suggests that changes in gene expression is specific to PPARγ targets and that deficit of PPARγ in neurons is not sufficient to compromise neuronal integrity including the presence of synapse-associated protein, synaptophysin that is often considered a surrogate marker for synapse density changes.

PPARγ-deficient in neurons renders neurons more susceptible to OGD-induced damage

To establish the relationship between PPARγ and neuronal susceptibility to ischemic injury, we first subjected the cultured neurons harvested from N-PPARγ-KO and control mice to OGD injury. The damage level was assessed by quantifying LDH and the oxidative stress to proteins (3-NT) and lipids (4-HNE). Also, we analyzed the neurite damage based on neurofilament loss (using Western blot) and gross morphological features of MAP2
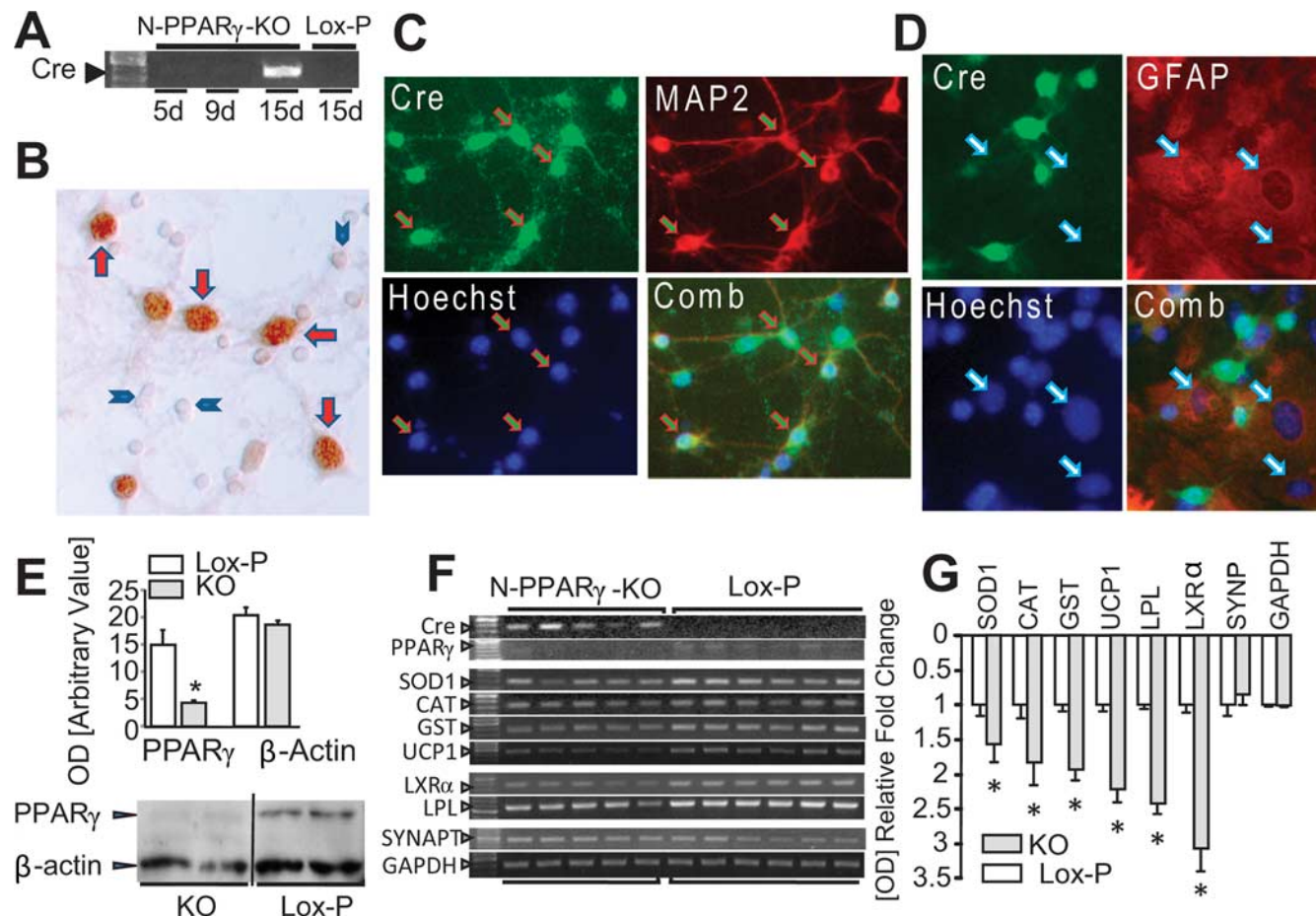
Figure 3. *A*, Photograph of RT-PCR gel demonstrating the Cre recombinase in neurons in culture that were produced from cortices of N-PPARγ-KO and control (Lox-P) mice, and immunohisto-chemistry (*B*) for Cre protein in neuron-glial coculture to show that the Cre is localized primarily to nuclei of cells with neuronal morphology (red arrows) but not in smaller neuroglia cells (blue arrowheads). *C*, *D*, Immunofluorescence demonstrating that Cre immunopositive cells in cultured neurons colocalize to MAP2 immunopositive (*C*) but not to GFAP immunopositive (*D*) cells in neuron-glia coculture. Cells were stained for Cre (green), MAP2 (neurons; red; *C*), GFAP (astroglia; red; *D*), and nuclei (Hoechst 33258; blue). Arrows in *C* identify cells positive for both Cre and MAP2, and arrows in *D* identify nuclei of GFAP-positive cells. Note that immunofluorescence for Cre does not overlap with the location of nuclei of GFAP-positive cells. *E*, Bar graph (*n* = 3) and a representative Western blot demonstrating PPARγ and β-actin protein level (determined via densitometrical analyses) in the neurons in culture that was generated from N-PPARγ-KO and the control (Lox-P) mice, at 15 d in culture. *F*, *G*, Quantification of mRNA expression in neurons in culture. *F*, Photographs of representative agarose gels of RT-PCR products and bar graph (*G*) showing densitometric quantification of RT-PCR products of the selected PPARγ-regulated genes in neuronal cultures generated from N-PPARγ-KO (KO) and control (Lox-P) mice, as measured after 15 d in culture. Synaptophysin (SYNAPT) and GAPDH were used as reference controls. The data are expressed as mean ± SEM (*n* = 5–6). In *E* and *G*, *$p \leq 0.05$ from control.

immunohistochemical study. All these assays were conducted at 24 h after OGD.

As predicted from the *in vivo* experiments, PPARγ-deficient neurons in response to OGD demonstrated more severe damage than the control neurons, as determined with assays for LDH release (Fig. 4*A*), morphological damage (Fig. 4*B*), neurofilament proteolysis (Fig. 4*C*), and oxidative stress (Fig. 4*F*). In agreement with the protective function of PPARγ, PPARγ-deficient neurons during exposure to OGD injury did not benefit from the treatment with PPARγ-activating agent, rosiglitazone, compared with the control neurons (Fig. 4*A*). Since OGD-mediated damage is at least in part associated with oxidative stress, we tested the hypothesis that PPARγ deficiency reduces neuron's ability to handle oxidative insult. Again, we used cultured neurons from N-PPARγ-KO mice and subjected them to a toxic level of hydrogen peroxide to model oxidative stress. In agreement with our postulate, PPARγ-deficient neurons were significantly more vulnerable to hydrogen peroxide-induced injury (Fig. 4*D*).

The neuron-selective PPARγ deletion did not appear to influence vulnerability of other brain cells to ischemia. Glia-enriched

cultures from N-PPARγ-KO mice subjected to OGD demonstrated undistinguishable level of damage compared with glia from the control mice (Fig. 4*E*).

Discussion

In this study, to gain more insight into the role of neuronal PPARγ, we generated neuronal-specific PPARγ knock-out mouse using LoxP–Cre system. These mutant mice are fully viable, have intact brain anatomy, and appear to develop normally. Because we used αCaM–KII promoter to achieve selective expression of Cre in neurons, we were likely able to retain undisturbed prenatal developmental process, since the induction of αCaM–KII promoter (used here to drive Cre expression; therefore mutation) does not occur until the early postnatal days (Burgin et al., 1990). In this study, we used a Tg–Cre-62 line of mice (Cui et al., 2004) which confines Cre recombinase expression to the forebrain, thus overlapping the middle cerebral artery territory (ischemia-affected aspect of the brain). Our results show that these PPARγ-deficient mice suffer more extensive damage in response to MCA/CCA occlusion, as revealed by increased volume of infarction and more pronounced functional deficit. This ag-
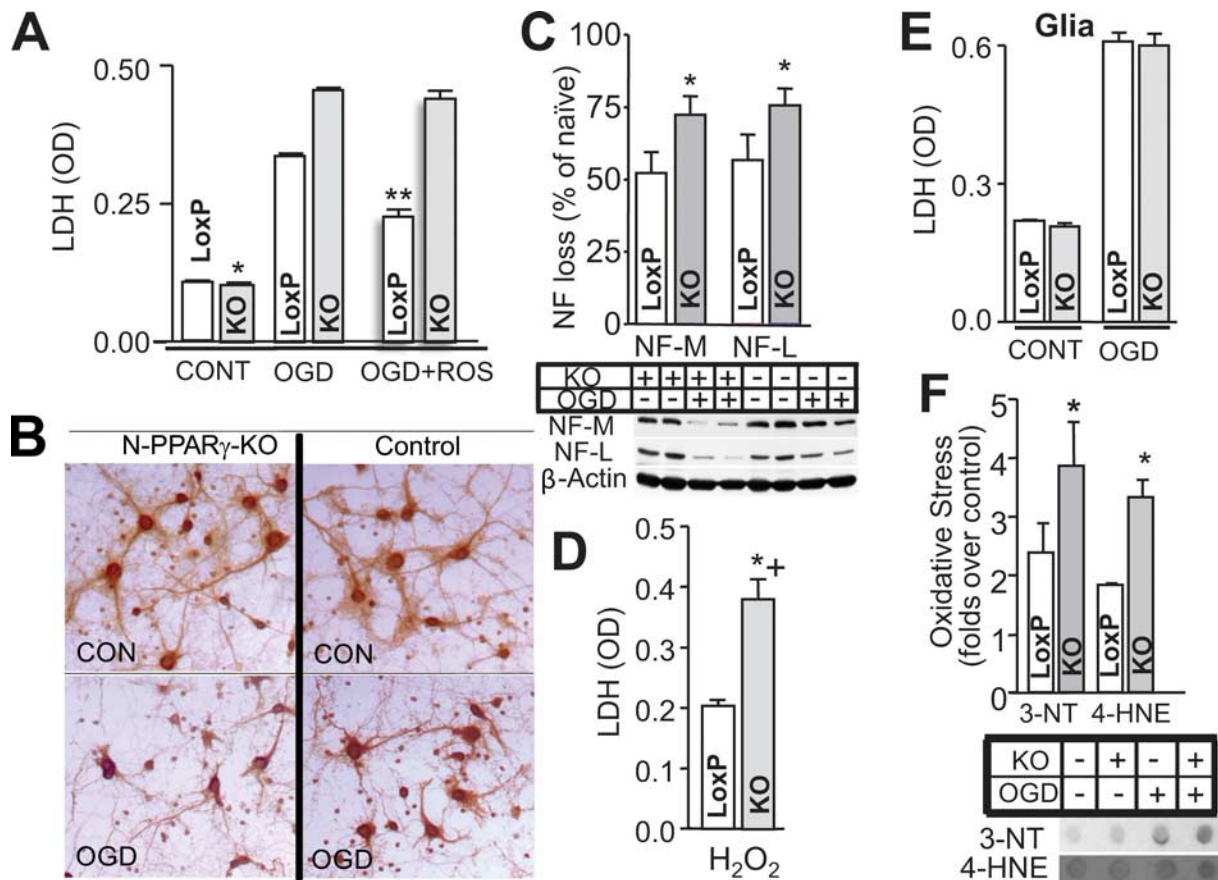
Figure 4. PPARγ deficiency renders neurons more vulnerable to damage. Neuron-enriched cultures (*A–D*, *F*) and glia-enriched cultures (*E*), generated from the control (LoxP) and N-PPARγ-KO (KO) mice were exposed to OGD, and the level of injury at 24 h was determined using LDH assay (*A*, *E*), loss of MAP2 integrity (*B*), oxidative stress (*F*; immuno-dot blot for 3′-NT and 4-HNE), and neurofilament hydrolysis (*C*; immunoblot for parent NF-L and NF-M protein). The effect of PPARγ agonist, rosiglitazone (ROS) on the OGD-induced injury in control and N-PPARγ-KO (KO) is also illustrated (*A*; last 2 bars). *D*, Bar graph illustrating LDH release from neurons in culture generated from LoxP and N-PPARγ-KO mice in response to H_2O_2-induced injury. In *A–F*, $n = 3$ independent experiments performed in triplicates (i.e., 3 culture well per experiment). *$p \leq 0.05$ from control; **$p < 0.05$ from KO and LoxP without ROS.

gravated damage is likely not attributable to altered cerebral perfusion, since laser Doppler data indicate that both the control and N-PPARγ-KO mice demonstrated similar level of blood perfusion reduction during MCA occlusion, as well as similar level of perfusion during the early postischemic phase. The lack of PPARγ involvement in cerebral perfusion in this study is consistent with our earlier and others' reports, showing that PPARγ-activating agents reduced ischemic damage without affecting intraischemic and early postischemic cerebral perfusion (Zhao et al., 2005; Victor et al., 2006; Tureyen et al., 2007). Although PPARγ is expressed by blood vessel cells where it plays diverse regulatory roles (Beyer et al., 2008), its function in context of acute stroke, at least with respect to blood flow regulation, appears to be limited. This suggests that some processes mediated via PPARγ within neurons protect neurons from ischemic damage. To test this hypothesis, we cultured cortical neurons from N-PPARγ-KO mice and probed their vulnerability by subjecting them to ischemia-like or oxidative stress injuries *in vitro*. In agreement with this hypothesis, PPARγ deficient neurons showed increased damage in response to ischemic or oxidative insult. Furthermore, in agreement with the prosurvival role of PPARγ, neurons deficient in PPARγ (in contrast to control neurons) did not benefit from the protective effect of PPARγ agonist, rosiglitazone. This experiment also indicates that rosiglitazone in fact requires PPARγ to provide neuroprotective effect. It is important to note that PPARγ deficiency does not affect the baseline

neuronal health (including presence of synaptic vesicle glycoprotein, synaptophysin), suggesting that the role of PPARγ in neurons is in maintaining cytoprotective/defense capacity of these cells. These results are consistent with our earlier study demonstrating that PPARγ antagonists (GW9662 and T0070907) at the concentration sufficient to reverse neuroprotective effect of PPARγ agonists did not cause neuronal injury (Zhao et al., 2006b).

Based on earlier studies with agents activating PPARγ from our and other laboratories, it was demonstrated that PPARγ mitigates inflammation after ischemic and hemorrhagic stroke (Sundararajan and Landreth, 2004; Sundararajan et al., 2005; Zhao et al., 2005, 2006a; Luo et al., 2006; Tureyen et al., 2007). Because inflammation is frequently recognized as a process contributing to the secondary brain damage (Garcia et al., 1994; del Zoppo et al., 2000; Aronowski and Hall, 2005), the anti-inflammatory effect of PPARγ agonists was proposed as a key mechanism underlying the beneficial role of PPARγ. However, in addition to its anti-inflammatory effect, PPARγ is known to regulate the expression of some important antioxidative enzymes such as catalase, SOD1, and GST (Yoo et al., 1999; Girnun et al., 2002; Park et al., 2004) that could effectively ameliorate oxidative stress, a recognized factor contributing to ischemic damage (Chan, 2001). Concurring with this notion, animals treated with PPARγ agonists demonstrated upregulated catalase and SOD1 in the injured brain (Park et al., 2004; Shimazu et al., 2005; Tureyen

et al., 2007; Zhao et al., 2007a), suggesting that antioxidative effect of PPARγ could indeed participate in protecting ischemic brain. Specifically, our study demonstrated that microglia in culture treated with PPARγ agonist increased expression of catalase, reduced generation of H_2O_2, and ultimately became less damaging toward neurons, as tested in neurons-microglia cocultures (Zhao et al., 2007a). Since both proinflammatory mediators and oxidative stress are the hallmarks of neurotoxicity via activated microglia (Gao et al., 2002; Qin et al., 2005), we initially proposed that inhibition of these microglia-mediated deleterious processes represents a key component of the beneficial effects of PPARγ.

Although the role of PPARγ activation in ameliorating the adverse effect of microglia is likely, our present study with PPARγ-deficient neurons strongly suggests that in addition to microglia, PPARγ is important in neuronal self-defense against ischemic and oxidative injuries. The analysis of gene expression in neurons cultured from N-PPARγ-KO mice showed that the disruption of PPARγ impairs expression of numerous genes that could improve neuronal resistance to ischemic and oxidative injury. First, PPARγ deficiency resulted in reduced expression of antioxidative catalase, SOD, and GST, thus providing a likely explanation for increased oxidative damage to proteins and lipids, as well as increased susceptibility of these neurons to oxygen–glucose deprivation or oxidative (H_2O_2) injuries. In addition to the gene products with antioxidative function, we also identified several other PPARγ-dependent genes with potential capacity to mediate anti-ischemic effects that were downregulated in neurons as a consequence of PPARγ deficiency. The first gene is the pleiotropic transcription factor, LXRα. Although we have not tested this possibility here, the reduced LXRα expression may have a direct impact on the increased ischemic vulnerability. The existing data suggest that LXRα possess prosurvival functions (Joseph et al., 2004) and that LXR agonist reduces damage after focal cerebral ischemia injury (Sironi et al., 2008). Another PPARγ-regulated gene reduced in PPARγ deficient neurons is LPL, an enzyme that functions to hydrolyze lipids and lipoproteins. Although the prosurvival function of LPL has not been studied, LPL is abundant in neurons and is upregulated in response to focal ischemia (Paradis et al., 2004). Further functional studies on the role of LPL in ischemia are warranted. Finally, we have identified a downregulation of UCP-1 in PPARγ-deficient neurons, confirming the regulatory role of PPARγ on uncoupling proteins (Kelly et al., 1998; Villarroya et al., 2007). Uncoupling proteins are the inner mitochondrial membrane proteins that dissipate the proton gradient capable of affecting free radical generation and cell viability in the context of ischemia and reperfusion, including in heart and brain (Hoerter et al., 2004; Chen et al., 2006). We also determined that neuronal deficiency in PPARγ did not impact nNOS, eNOS, and iNOS expression in cultured neurons (data not included).

Our analysis of mouse brain after cerebral ischemia showed that selective neuronal PPARγ deficiency causes significant increase in the infract volume, indicating that the tissue damage is embracing not only neurons but also other non-neuronal cells. The reason why change in neuronal genotype/phenotype affects susceptibility of other than neurons cells to ischemic damage is not clear, although well documented in the existing literature. For instance, excitotoxic insult (e.g., intracerebral injection of NMDA) preferentially damages neurons, although the lesion produced around the area of excitotoxin injection consists of mixed cell loss. Additionally, studies with other cell-specific mutant mice tested for ischemic vulnerability showed that neuronal-selective inhibition of inhibitor κB kinase-β (Herrmann et al.,

2004) reduced overall infarct size, whereas neuronal-selective hypoxia-inducible factor-1α deficiency leads to increase infarct volume (Baranova et al., 2007). One possible explanation for such inclusive cell loss is that the dying neurons adversely impact surrounding cells by the release/spillage of the cytotoxic content after their injury/lysis. Thus, in N-PPARγ-KO mice, ischemia-induced death of more vulnerable neurons in the transitional ischemic zone (distal penumbra), attributable to PPARγ deficiency, may injure adjacent cells, causing infarct volume to enlarge. Alternatively, loss of non-neuronal cells may suggest the instrumental role of neurons in maintaining integrity of all the cells comprising the neurovascular unit. Taken as a whole, it is important to stress that our present study provides additional evidence that selective change in neuronal resistance to ischemia adversely affects survival of all brain cells in ischemia-endangered zone.

Since estrogen receptors are linked to neuroprotection and anti-ischemic effect (McCullough et al., 2001), and PPARγ directly modulates transactivation of estrogen receptor-α (Houston et al., 2003), we were interested in establishing whether PPARγ deficiency may have different effect on ischemic vulnerability in male versus female mice. Our data demonstrate that PPARγ deficiency increases ischemic brain damage in both genders, suggesting that changes in estrogen receptor expression or other gender-related cellular processes do not likely contribute to the overall increased vulnerability of N-PPARγ-KO mice.

In conclusion, our data unveil a previously unclear neuroprotective role for PPARγ in neuronal self-protection from insults such as ischemia and oxidative stress. The present data indicate that PPARγ in neurons is not essential for normal neuronal well being, but it plays an important role in protecting neurons from damage by ischemic and oxidative injury. This cytoprotective role of PPARγ is likely attributable to induction of multiple prosurvival gene products and their multimodal effects. Finally, our data suggest that the neuroprotective function of PPARγ reinforces the growing body of evidence recognizing PPARγ as a logical target for neurological diseases with pathogenesis including ischemia and/or oxidative stress.

References

Akiyama TE, Sakai S, Lambert G, Nicol CJ, Matsusue K, Pimprale S, Lee YH, Ricote M, Glass CK, Brewer HB Jr, Gonzalez FJ (2002) Conditional disruption of the peroxisome proliferator-activated receptor gamma gene in mice results in lowered expression of ABCA1, ABCG1, and apoE in macrophages and reduced cholesterol efflux. Mol Cell Biol 22:2607–2619.

Aronowski J, Hall CE (2005) New horizons for primary intracerebral hemorrhage treatment: experience from preclinical studies. Neurol Res 27:268–279.

Aronowski J, Strong R, Grotta JC (1997) Reperfusion injury: demonstration of brain damage produced by reperfusion after transient focal ischemia in rats. J Cereb Blood Flow Metab 17:1048–1056.

Aronowski J, Cho KH, Strong R, Grotta JC (1999) Neurofilament proteolysis after focal ischemia; when do cells die after experimental stroke? J Cereb Blood Flow Metab 19:652–660.

Aronowski J, Grotta JC, Strong R, Waxham MN (2000) Interplay between the gamma isoform of PKC and calcineurin in regulation of vulnerability to focal cerebral ischemia. J Cereb Blood Flow Metab 20:343–349.

Baranova O, Miranda LF, Pichiule P, Dragatsis I, Johnson RS, Chavez JC (2007) Neuron-specific inactivation of the hypoxia inducible factor 1α increases brain injury in a mouse model of transient focal cerebral ischemia. J Neurosci 27:6320–6332.

Berger J, Moller DE (2002) The mechanisms of action of PPARs. Annu Rev Med 53:409–435.

Beyer AM, Baumbach GL, Halabi CM, Modrick ML, Lynch CM, Gerhold TD, Ghoneim SM, de Lange WJ, Keen HL, Tsai YS, Maeda N, Sigmund CD, Faraci FM (2008) Interference with PPARgamma signaling causes cere-

bral vascular dysfunction, hypertrophy, and remodeling. Hypertension 51:867–871.

Burgin KE, Waxham MN, Rickling S, Westgate SA, Mobley WC, Kelly PT (1990) *In situ* hybridization histochemistry of Ca²⁺/calmodulin-dependent protein kinase in developing rat brain. J Neurosci 10:1788–1798.

Chan PH (2001) Reactive oxygen radicals in signaling and damage in the ischemic brain. J Cereb Blood Flow Metab 21:2–14.

Chen SD, Wu HY, Yang DI, Lee SY, Shaw FZ, Lin TK, Liou CW, Chuang YC (2006) Effects of rosiglitazone on global ischemia-induced hippocampal injury and expression of mitochondrial uncoupling protein 2. Biochem Biophys Res Commun 351:198–203.

Chinetti G, Fruchart JC, Staels B (2000) Peroxisome proliferator-activated receptors (PPARs): nuclear receptors at the crossroads between lipid metabolism and inflammation. Inflamm Res 49:497–505.

Cui Z, Wang H, Tan Y, Zaia KA, Zhang S, Tsien JZ (2004) Inducible and reversible NR1 knockout reveals crucial role of the NMDA receptor in preserving remote memories in the brain. Neuron 41:781–793.

Cui Z, Lindl KA, Mei B, Zhang S, Tsien JZ (2005) Requirement of NMDA receptor reactivation for consolidation and storage of nondeclarative taste memory revealed by inducible NR1 knockout. Eur J Neurosci 22:755–763.

Dello Russo C, Gavrilyuk V, Weinberg G, Almeida A, Bolanos JP, Palmer J, Pelligrino D, Galea E, Feinstein DL (2003) Peroxisome proliferator-activated receptor gamma thiazolidinedione agonists increase glucose metabolism in astrocytes. J Biol Chem 278:5828–5836.

del Zoppo G, Ginis I, Hallenbeck JM, Iadecola C, Wang X, Feuerstein GZ (2000) Inflammation and stroke: putative role for cytokines, adhesion molecules and iNOS in brain response to ischemia. Brain Pathol 10:95–112.

Felberg RA, Grotta JC, Shirzadi AL, Strong R, Narayana P, Hill-Felberg SJ, Aronowski J (2002) Cell death in experimental intracerebral hemorrhage: the "black hole" model of hemorrhagic damage. Ann Neurol 51:517–524.

Forman BM, Tontonoz P, Chen J, Brun RP, Spiegelman BM, Evans RM (1995) 15-Deoxy-delta 12, 14-prostaglandin J2 is a ligand for the adipocyte determination factor PPAR gamma. Cell 83:803–812.

Gao HM, Jiang J, Wilson B, Zhang W, Hong JS, Liu B (2002) Microglial activation-mediated delayed and progressive degeneration of rat nigral dopaminergic neurons: relevance to Parkinson's disease. J Neurochem 81:1285–1297.

Garcia JH, Liu KF, Yoshida Y, Lian J, Chen S, del Zoppo GJ (1994) Influx of leukocytes and platelets in an evolving brain infarct (Wistar rat). Am J Pathol 144:188–199.

Giannini S, Serio M, Galli A (2004) Pleiotropic effects of thiazolidinediones: taking a look beyond antidiabetic activity. J Endocrinol Invest 27:982–991.

Girnun GD, Domann FE, Moore SA, Robbins ME (2002) Identification of a functional peroxisome proliferator-activated receptor response element in the rat catalase promoter. Mol Endocrinol 16:2793–2801.

He W, Barak Y, Hevener A, Olson P, Liao D, Le J, Nelson M, Ong E, Olefsky JM, Evans RM (2003) Adipose-specific peroxisome proliferator-activated receptor gamma knockout causes insulin resistance in fat and liver but not in muscle. Proc Natl Acad Sci U S A 100:15712–15717.

Herrmann O, Baumann B, Schwaninger M (2004) Inhibition of IKK-2 reduces infarct size in a model of cerebral ischemia. Paper presented at the 10th International Symposium on Pharmacology of Cerebral Ischemia, Marburg, Germany, December.

Hevener AL, He W, Barak Y, Le J, Bandyopadhyay G, Olson P, Wilkes J, Evans RM, Olefsky J (2003) Muscle-specific Pparg deletion causes insulin resistance. Nat Med 9:1491–1497.

Hoerter J, Gonzalez-Barroso MD, Couplan E, Mateo P, Gelly C, Cassard-Doulcier AM, Diolez P, Bouillaud F (2004) Mitochondrial uncoupling protein 1 expressed in the heart of transgenic mice protects against ischemic-reperfusion damage. Circulation 110:528–533.

Houston KD, Copland JA, Broaddus RR, Gottardis MM, Fischer SM, Walker CL (2003) Inhibition of proliferation and estrogen receptor signaling by peroxisome proliferator-activated receptor gamma ligands in uterine leiomyoma. Cancer Res 63:1221–1227.

Jiang C, Ting AT, Seed B (1998) PPAR-gamma agonists inhibit production of monocyte inflammatory cytokines. Nature 391:82–86.

Joseph SB, Bradley MN, Castrillo A, Bruhn KW, Mak PA, Pei L, Hogenesch J,

O'connell RM, Cheng G, Saez E, Miller JF, Tontonoz P (2004) LXR-dependent gene expression is important for macrophage survival and the innate immune response. Cell 119:299–309.

Kelly LJ, Vicario PP, Thompson GM, Candelore MR, Doebber TW, Ventre J, Wu MS, Meurer R, Forrest MJ, Conner MW, Cascieri MA, Moller DE (1998) Peroxisome proliferator-activated receptors gamma and alpha mediate in vivo regulation of uncoupling protein (UCP-1, UCP-2, UCP-3) gene expression. Endocrinology 139:4920–4927.

Kelly PT, Shields S, Conway K, Yip R, Burgin K (1987) Developmental changes in calmodulin-kinase II activity at brain synaptic junctions: alterations in holoenzyme composition. J Neurochem 49:1927–1940.

Kim DH, Zhao X, Tu CH, Casaccia-Bonnefil P, Chao MV (2004) Prevention of apoptotic but not necrotic cell death following neuronal injury by neurotrophins signaling through the tyrosine kinase receptor. J Neurosurg 100:79–87.

Kliewer SA, Forman BM, Blumberg B, Ong ES, Borgmeyer U, Mangelsdorf DJ, Umesono K, Evans RM (1994) Differential expression and activation of a family of murine peroxisome proliferator-activated receptors. Proc Natl Acad Sci U S A 91:7355–7359.

Kliewer SA, Lenhard JM, Willson TM, Patel I, Morris DC, Lehmann JM (1995) A prostaglandin J2 metabolite binds peroxisome proliferator-activated receptor gamma and promotes adipocyte differentiation. Cell 83:813–819.

Lehmann JM, Moore LB, Smith-Oliver TA, Wilkison WO, Willson TM, Kliewer SA (1995) An antidiabetic thiazolidinedione is a high affinity ligand for peroxisome proliferator-activated receptor gamma (PPAR gamma). J Biol Chem 270:12953–12956.

Luo Y, Yin W, Signore AP, Zhang F, Hong Z, Wang S, Graham SH, Chen J (2006) Neuroprotection against focal ischemic brain injury by the peroxisome proliferator-activated receptor-gamma agonist rosiglitazone. J Neurochem 97:435–448.

Mangelsdorf DJ, Thummel C, Beato M, Herrlich P, Schütz G, Umesono K, Blumberg B, Kastner P, Mark M, Chambon P, Evans RM (1995) The nuclear receptor superfamily: the second decade. Cell 83:835–839.

McCullough LD, Alkayed NJ, Traystman RJ, Williams MJ, Hurn PD (2001) Postischemic estrogen reduces hypoperfusion and secondary ischemia after experimental stroke. Stroke 32:796–802.

Olson NJ, Massé T, Suzuki T, Chen J, Alam D, Kelly PT (1995) Functional identification of the promoter for the gene encoding the alpha subunit of calcium/calmodulin-dependent protein kinase II. Proc Natl Acad Sci U S A 92:1659–1663.

Ou Z, Zhao X, Labiche LA, Strong R, Grotta JC, Herrmann O, Aronowski J (2006) Neuronal expression of peroxisome proliferator-activated receptor-gamma (PPARgamma) and 15d-prostaglandin J(2)-Mediated protection of brain after experimental cerebral ischemia in rat. Brain Res 1096:196–203.

Paradis E, Clavel S, Julien P, Murthy MR, de Bilbao F, Arsenijevic D, Giannakopoulos P, Vallet P, Richard D (2004) Lipoprotein lipase and endothelial lipase expression in mouse brain: regional distribution and selective induction following kainic acid-induced lesion and focal cerebral ischemia. Neurobiol Dis 15:312–325.

Park EY, Cho IJ, Kim SG (2004) Transactivation of the PPAR-responsive enhancer module in chemopreventive glutathione S-transferase gene by the peroxisome proliferator-activated receptor-gamma and retinoid X receptor heterodimer. Cancer Res 64:3701–3713.

Pereira MP, Hurtado O, Cárdenas A, Alonso-Escolano D, Boscá L, Vivancos J, Nombela F, Leza JC, Lorenzo P, Lizasoain I, Moro MA (2005) The nonthiazolidinedione PPARgamma agonist L-796,449 is neuroprotective in experimental stroke. J Neuropathol Exp Neurol 64:797–805.

Qin L, Liu Y, Qian X, Hong JS, Block ML (2005) Microglial NADPH oxidase mediates leucine enkephalin dopaminergic neuroprotection. Ann N Y Acad Sci 1053:107–120.

Ricote M, Li AC, Willson TM, Kelly CJ, Glass CK (1998) The peroxisome proliferator-activated receptor-gamma is a negative regulator of macrophage activation. Nature 391:79–82.

Rohn TT, Wong SM, Cotman CW, Cribbs DH (2001) 15-deoxy-delta12,14-prostaglandin J2, a specific ligand for peroxisome proliferator-activated receptor-gamma, induces neuronal apoptosis. Neuroreport 12:839–843.

Romera C, Hurtado O, Mallolas J, Pereira MP, Morales JR, Romera A, Serena J, Vivancos J, Nombela F, Lorenzo P, Lizasoain I, Moro MA (2007) Ischemic preconditioning reveals that GLT1/EAAT2 glutamate transporter is

a novel PPARgamma target gene involved in neuroprotection. J Cereb Blood Flow Metab 27:1327–1338.

Scholz WK, Baitinger C, Schulman H, Kelly PT (1988) Developmental changes in Ca²⁺/calmodulin-dependent protein kinase II in cultures of hippocampal pyramidal neurons and astrocytes. J Neurosci 8:1039–1051.

Shimazu T, Inoue I, Araki N, Asano Y, Sawada M, Furuya D, Nagoya H, Greenberg JH (2005) A peroxisome proliferator-activated receptor-gamma agonist reduces infarct size in transient but not in permanent ischemia. Stroke 36:353–359.

Sironi L, Mitro N, Cimino M, Gelosa P, Guerrini U, Tremoli E, Saez E (2008) Treatment with LXR agonists after focal cerebral ischemia prevents brain damage. FEBS Lett 582:3396–3400.

Stumvoll M, Häring HU (2002) Glitazones: clinical effects and molecular mechanisms. Ann Med 34:217–224.

Sundararajan S, Landreth GE (2004) Antiinflammatory properties of PPARgamma agonists following ischemia. Drug News Perspect 17:229–236.

Sundararajan S, Gamboa JL, Victor NA, Wanderi EW, Lust WD, Landreth GE (2005) Peroxisome proliferator-activated receptor-gamma ligands reduce inflammation and infarction size in transient focal ischemia. Neuroscience 130:685–696.

Swanson RA, Morton MT, Tsao-Wu G, Savalos RA, Davidson C, Sharp FR (1990) A semiautomated method for measuring brain infarct volume [see comments]. J Cereb Blood Flow Metab 10:290–293.

Tsien JZ, Chen DF, Gerber D, Tom C, Mercer EH, Anderson DJ, Mayford M, Kandel ER, Tonegawa S (1996) Subregion- and cell type-restricted gene knockout in mouse brain. Cell 87:1317–1326.

Tureyen K, Kapadia R, Bowen KK, Satriotomo I, Liang J, Feinstein DL, Vemuganti R (2007) Peroxisome proliferator-activated receptor-gamma agonists induce neuroprotection following transient focal ischemia in normotensive, normoglycemic as well as hypertensive and type-2 diabetic rodents. J Neurochem 101:41–56.

Uryu S, Harada J, Hisamoto M, Oda T (2002) Troglitazone inhibits both post-glutamate neurotoxicity and low-potassium-induced apoptosis in cerebellar granule neurons. Brain Res 924:229–236.

Victor NA, Wanderi EW, Gamboa J, Zhao X, Aronowski J, Deininger K, Lust WD, Landreth GE, Sundararajan S (2006) Altered PPARgamma expression and activation after transient focal ischemia in rats. Eur J Neurosci 24:1653–1663.

Villarroya F, Iglesias R, Giralt M (2007) PPARs in the control of uncoupling proteins gene expression. PPAR Res 2007:74364.

Yoo HY, Chang MS, Rho HM (1999) Induction of the rat Cu/Zn superoxide dismutase gene through the peroxisome proliferator-responsive element by arachidonic acid. Gene 234:87–91.

Zhao X, Zhang Y, Strong R, Grotta JC, Aronowski J (2006a) 15d-Prostaglandin J(2) activates peroxisome proliferator-activated receptor-gamma, promotes expression of catalase, and reduces inflammation, behavioral dysfunction, and neuronal loss after intracerebral hemorrhage in rats. J Cereb Blood Flow Metab 26:811–820.

Zhao X, Ou Z, Grotta JC, Waxham N, Aronowski J (2006b) Peroxisome-proliferator-activated receptor-gamma (PPARgamma) activation protects neurons from NMDA excitotoxicity. Brain Res 1073–1074:460–469.

Zhao X, Sun G, Zhang J, Strong R, Song W, Gonzales N, Grotta JC, Aronowski J (2007a) Hematoma resolution as a target for intracerebral hemorrhage treatment: role for PPARg in microglia/macrophage. Ann Neurol 61:352–362.

Zhao X, Sun G, Zhang J, Strong R, Dash PK, Kan YW, Grotta JC, Aronowski J (2007b) Transcription factor Nrf2 protects the brain from damage produced by intracerebral hemorrhage. Stroke 38:3280–3286.

Zhao Y, Patzer A, Gohlke P, Herdegen T, Culman J (2005) The intracerebral application of the PPARgamma-ligand pioglitazone confers neuroprotection against focal ischaemia in the rat brain. Eur J Neurosci 22:278–282.